UNIVERSITY OF BATH

University of Bath

WEAK SIGNAL DETECTION BASED ON TWO DIMENSIONAL STOCHASTIC RESONANCE

Leonardo Barbini *, *Matthew O. T. Cole, Andrew J. Hillis, Jonathan L. du Bois*

University of Bath
Department of Mechanical Engineering
Claverton Down, Bath, BA2 7AY UK

ABSTRACT

The analysis of vibrations from rotating machines gives information about their faults. From the signal processing perspective a significant problem is the detection of weak signals embedded in strong noise. Stochastic resonance (SR) is a mechanism where noise is not suppressed but exploited to trigger the synchronization of a non-linear system and in its one-dimensional form has been recently applied to vibration analysis. This paper focuses on the use of SR in a two-dimensional system of gradient type for detection of weak signals submerged in Gaussian noise. Comparing the traditional one-dimensional system and the two-dimensional used here, this paper shows that the latter can offer a more sensitive means of detection. An alternative metric is proposed to assess the output signal quality, requiring no *a priori* knowledge of the signal to be detected, and it is shown to offer similar results to the more conventional signal-to-noise ratio.

Index Terms— stochastic resonance, weak signal detection, non linear signal processing

1. INTRODUCTION

The response of a non-linear system to both the effects of noise and a periodic signal can result in a phenomenon of synchronization: stochastic resonance (SR) [1]. In the field of mechanical engineering a problem of great importance is that under operating conditions of many mechanical equipment, signals carrying useful information are submerged by heavy background noise. Conventional methods for the enhancement of the useful signal, so that it can be detected, consist of filtering or masking the noise [2,3] while in the SR mechanism the noise is used to enhance the signal, reducing the risk of losing the information of interest. In this context the flow of the detection scheme is as follows. The sum of periodic aperiodic or impact signals [4] and an heavy noise is preprocessed [4,5] and taken as the input of the non linear system, usually a 1D double well. Then will start an algorithm for tuning the parameters of this non-linear system, in order to trigger the SR mechanism. For each combination of the parameters, the output signal will be collected and evaluated

with certain criteria, such as maximization of the weighted kurtosis index (KC) or of the signal-to-noise ratio (SNR), so that the best output is found and the signal of interest is detected [4]. The assumption of the adiabatic approximation for the SR mechanism, i.e. small values of frequency, amplitude and noise variance, can be avoided [5] hence in practical applications also high frequency-amplitude signals can be detected (henceforth "large parameter SR"). It is worth noticing that in the above mentioned detection scheme two key roles are the type of non linearity of the system and the optimization criteria; the former because it determines the set of variables that one is able to tune, the latter because it decides the values of those variables.

In the present paper we investigate both of the above mentioned aspects, firstly we will show how switching to a non linear system in more than one dimension will allow us to tune another parameter. Barbini *et al.* [6] investigated the effect of the addition of another degree of freedom to the usual bistable system used for the SR mechanism. It was observed a dependence of the output signal on the coupling constant, due to a change in the transition path among the stable points. Then the number of parameters which can be tuned increases, now being: the height of the potential barrier, the position of the stable points and also the coupling constant. One is tempted to think that for the same input signal, after the tuning process of the parameters, the output of the SR will be the same in the two cases. We investigate this question, comparing the best result of the 2D non-linear system with the mono-dimensional one, for the same input signal when the parameters are tuned in the same range of values. Secondly we propose a new criterion for selecting the best values of the three tuning parameters. Instead of looking at a time-frequency transformation we evaluate the degree of synchronization of the output signal using directly the distribution of the mean residence time in the stable points of the non linear system.

The paper is structured as follows. In section 2 we provide a description of the two dimensional non linear system, as well as the rescaling for extending the large parameter SR to this model. In section 3 we test the efficiency of the new tuning criteria for the parameters, detecting signals using the 1D model. In section 4 we show the dependence of the output in the 2D model on the coupling constant and comparing with

---

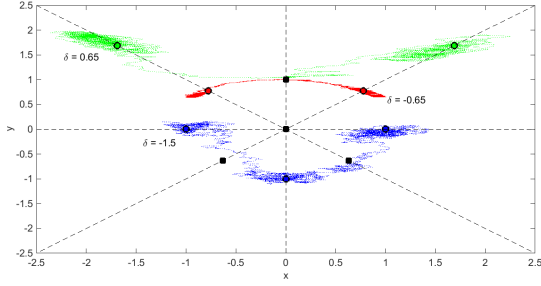*Corresponding author. Email address: l.barbini@bath.ac.uk

Fig. 1. Paths on the $x - y$ plane for different values of δ: blue -1.5, red -0.65 and green 0.65. Circles and squares are respectively stable and unstable steady states

the results obtained in the 1D case. Conclusions and an outlook for future development are given in the final section.

2. NORMALIZED TWO DIMENSIONAL SR

Let us consider the dynamical system associated to the following potential:

$$U\left(x, y\right) = -\frac{a}{2}\left(x^2 + y^2\right) + \frac{b}{4}\left(x^4 + y^4\right) - \frac{\delta}{2}\left(x^2 y^2\right) \quad (1)$$

where a, b, δ are real positive numbers. This potential is the generalization of the one studied in [6], where $a = b = 1$. Throughout the paper we will consider the inertia small compared to other dynamical components.

The origin is an unstable steady point so that if we consider the effect of small fluctuations to the motionless state, i.e. noise, we will observe the system to stabilize in one of the minima, then for increasing values of the fluctuations we will have random transition between those minima symmetrically displaced in the quadrants. The system is two dimensional hence, differently from the usual double well, as a function of a, b, δ we have the possibility to have saddle points as unstable steady states and curved transition paths in the (x, y) plane. Respectively a, b define the height of the potential barrier between the stable steady states and their positions; δ is the coupling. Whether transitions will take place among saddle points or the maxima as well as the rate, depend on both the height of the potential barrier and on the curvature of the potential landscape [7]. In Fig.1 we show the displacement of the steady states and the transitions paths for different values of the coupling in the case $a = b = 1$. In green ($\delta = 0.65$) and red ($\delta = -0.65$) stable states lie on the axes of the plane and transitions occur through an unstable steady state at $(0, 1)$. Due to the symmetry of (1) such transitions could take place also between the $I-II, II-III$ and $III-IV$ quadrants (not shown). When the value of the coupling constant is lower than $\delta < -1$ there is a change in the stability of the steady states of the potential, in Fig.1 we show in blue transitions in the case $\delta = -1.5$. It can be noticed that unstable steady states are
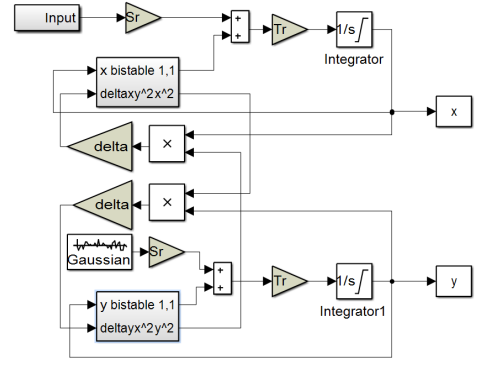

Fig. 2. Model of the two dimensional SR detector

now situated on the axes of the plane while steady states are at $(0, -1)$ and $(1, 0)$ respectively. The same considerations on the symmetry apply in this case.

Let us consider now the effect of a periodic forcing on the dynamical system of stochastic differential equations obtained from the potential defined in (1). We add a periodic component $A cos(\omega t)$, of amplitude A and frequency ω, on the first of the two equations:

$$\begin{cases} dx = \left[ax - bx^3 + \delta xy^2 + A cos(\omega t)\right] dt + \varepsilon_x^{1/2} dw_x \\ dy = \left(ay - by^3 + \delta yx^2\right) dt + \varepsilon_y^{1/2} dw_y \end{cases}$$
$$(2)$$

where $dw_{(.)}$ are independent Wiener processes and $\varepsilon_{(.)}$ the variances of the noise. The effect of the periodic component in the first of (2) is that of modulate the potential (1), i.e. the height of the barrier between stable states changes implying a periodicity in the transition rates [1]. This synchronization phenomenon is the result of the cooperative effect of the periodic component and the noise, hence the transition rates are a function of both A, ω, ε, as well as the parameters of the non linear system a, b, δ.

The theory of stochastic differential equations provides an estimate of the mean exit time from the basins of attractions of the stable points in the limit of small parameters A, ω, ε [1,7]. Nevertheless for a good use of SR in signal detection these limitations on the characteristic of the analysed signal must be avoided. Then following [5] we extend the rescale transformation to (2). For $a, b > 0$ we take a constant $k > 0$, we let and $\hat{x} = x\sqrt{b/a}, \hat{y} = y\sqrt{b/a}, \hat{\delta} = \delta/b, \hat{t} = t/k$; hence (2) reduces to the following system which preserves the gradient type structure:

$$\begin{cases} d\hat{x} = T_R \left\{ \left(\hat{x} - \hat{x}^3 + \hat{\delta}\hat{x}\hat{y}^2\right) d\hat{t} + S_R \left[A cos\left(\Omega\hat{t}\right) d\hat{t} + \varepsilon_x^{1/2} d\hat{w}_x\right] \right\} \\ d\hat{y} = T_R \left[\left(\hat{y} - \hat{y}^3 + \hat{\delta}\hat{y}\hat{x}^2\right) d\hat{t} + S_R \varepsilon_y^{1/2} d\hat{w}_y\right] \end{cases}$$
$$(3)$$

where $T_R = ak$ is the time rescale, $S_R = b^{1/2} a^{-3/2}$ is the spatial rescale, $\Omega = k\omega$ is the new signal frequency and the Wiener process $d\hat{w}$ keeps the statistical conditions $\langle d\hat{w}\rangle = 0, \langle d\hat{w}, d\hat{w}'\rangle = \delta(\hat{t}-\hat{t}')$; in the following we will omit the $\hat{\cdot}$ for
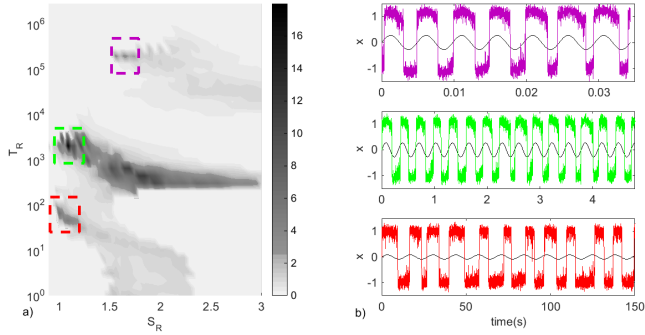
Fig. 3. a) contour plot of r_τ for the 1D detector; b) three output signals obtained for the values of S_R, T_R giving the maxima of r_τ. In black the periodic components of the input: top $(A_3, \omega_3) = (0.2794, 203.6811)$, middle $(A_2, \omega_2) = (0.2727, 3.1748)$ and bottom $(A_1, \omega_1) = (0.0845, 0.0741)$
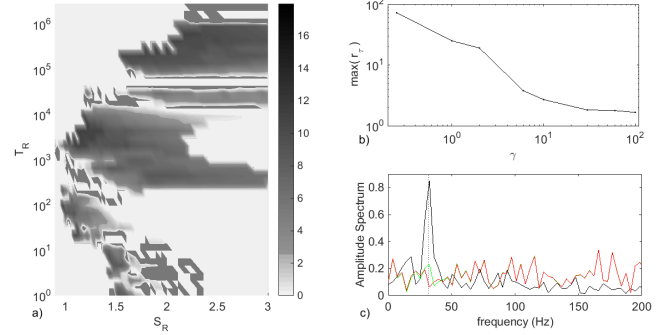

Fig. 4. a) contour plot of SNR for the 1D detector; b) dependence of maximum of r_τ on the amplitude $\gamma \varepsilon_x^{1/2}$ of the input noise; c) amplitude spectra of input noise (red) for $\gamma = 6, \varepsilon_x = (5.4976)^2$, input noise plus sinusoid (green) in the case $(A, \omega) = (0.2749, 31.6426)$, output of 1D SR detector (black)

simplicity. In practical application of SR as a signal detection method, the input of the nonlinear system is a noisy signal and the main objective is to analyze whether a periodic component is present or not. Referring to (3) the input is the sum of the last two terms of the first equation, with unknown A, ω, ε_x. In system (3) the values of the frequency and of the amplitude of the input signal can be taken without constraints, being multiplied respectively by S_R, k and the position of the stable points in the (x, y) plane and the height of the potential barrier are now fixed, being now the dependence on a, b in $S_R(a, b)$. The detection problem is then reduced to finding the values of T_R, S_R, δ providing a 2D SR mechanism giving an output signal x which shows a transition rate highly synchronized to the periodic component of the input. According to the order of magnitude expected for the frequency and amplitude of the periodic component we will decide the range of values for the parameters T_R and S_R. Then we will test all those for a selected range of values of the coupling constant δ, so that we will have to select the best output from a total number of $n_{T_R} \times n_{S_R} \times n_\delta$. In the present paper we propose to study directly the distribution of the transition rates τ i.e. the exit times from the basins of attraction of stable steady states of (3). Those are obtained from the array of the times of the x-mode zero crossing for each of the output signals. When the system is out of resonance, the times of the transitions between stable states are random, then the distribution of τ depicts no structure and decays exponentially. In [8] Benzi *et al.* showed that the moments for τ are given by:

$$\langle \tau^n \rangle \approx n! \, \langle \tau \rangle^n \qquad (4)$$

In contrast, when we have SR the distribution of τ is peaked at the time being half period of the periodic forcing. In the present paper we use the ratio r_τ between the square of the mean and the variance of τ in order to evaluate the degree of the SR: $r_\tau = \langle \tau \rangle^2 / \left(\langle \tau^2 \rangle - \langle \tau \rangle^2 \right)$. The control parameter

r_τ has to be independent from the time scale at which it is evaluated; this is why it is normalized with the mean here. According to (4) when the system shows completely random jumps r_τ reaches the value 1, while in the SR case $r_\tau \to \infty$ for a perfect identification of the signal frequency. The detection ends finding the maximum from all the r_τ, the measure of success of the procedure is that of detecting the signal carrying the useful information, for which the ratio $r = A/\varepsilon_x$ is the lowest.

3. NUMERICAL RESULTS: TEST OF R_τ

In this section we test the use of r_τ as a control parameter for the SR, all our numerical results are taken from a Simulink model reproducing system (3), the model is shown in Fig.2, the input block models the addition of periodic signals and a Gaussian noise:

$$Input = \sum_n A_n sin \left(\omega_n t \right) + \varepsilon_x^{1/2} \eta(t) \qquad (5)$$

being $\eta(t) = dw/dt$, and n the number of components. Within this section we restrict our analysis to the 1D system, i.e the first equation of (3) with $\delta = 0$. We test the model with an input signal constructed as follows: $n = 3$; the amplitudes and frequencies of the periodic components are chosen randomly in the ranges of values 0.01 to 1 and 0.001 to 1000 Hz respectively; the variance of the noise is taken as the result of multiplication of the highest of the A_i for a random number in the range 5 to 10 so that we ensure that the periodic signals are heavily buried into noise. The following values for the input signal were found: $(A_1, \omega_1) = (0.0845, 0.0741), (A_2, \omega_2) = (0.2727, 3.1748), (A_3, \omega_3) = (0.2794, 203.6811)$ and $\varepsilon_x = (2.3497)^2$. The tuning parameters T_R, S_R are tested in the range 1 to 10^6, 0.01 to 15 respectively and we decide increment steps so that we end up in a matrix of dimensions $n_{T_R} \times n_{S_R} = 40 \times 250$. In the simulations for each T_R we
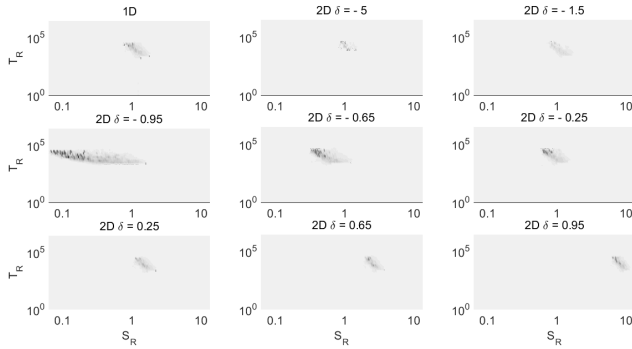
Fig. 5. contour plot of r_τ: top left 1D detector, all the others are for the 2D detector with different δ

Fig. 6. maxima of r_τ for the 2D detector (red) as a function of δ: a)$\gamma = 0.25$, b) $\gamma = 1$, c) $\gamma = 2$, d) $\gamma = 6$; in blue 1D

change both the integration time step $dt = 2^{-6}/T_R$ and the time length of the analyzed signals $L = 10000/T_R$, while we keep fixed the number of samples and we sub-sample the output of 27, so that we end up with signals of 5000 samples. In Fig.3(a) we show the contour plot of the values of r_τ for each of the tuning parameter, we have recognized the areas, red green and purple, for the peaks corresponding to the three periodic components of the input signal. In Fig.3(b) we show a comparison between the periodic components, black signals, and the three output x obtained setting S_R, T_R as for the maxima of r_τ; the time scales of the plots are different and after the SR we can appreciate the time decomposition of the three components of the input. We show the classical signal to noise ratio (SNR) metric calculated for the output values for each of the tuning parameter in Fig.4(a), SNR is defined as the ratio between the power of the spectral line at the periodic input frequency and that of the noise background [5], we notice that the areas corresponding to the three input frequencies are visible and comparable with those of r_τ and that a good comparison is possible. In Fig.3(a) we notice the displacement of the peaks in the S_R dimension due both to the ratio $r_i = A_i/\varepsilon_x$ and the superposition of the signals at different frequencies. In order to quantify the dependence of r_τ on the ratio r without such a superposition we test an input signal where there is only one periodic component, $n = 1$ in (5). Following the above mentioned construction procedure we found the following values for the amplitude and frequency $(A, \omega) = (0.2749, 31.6426)$ and for the variance $\varepsilon_x = (5.4976)^2$. Then we modify the ratio r multiplying the variance for $\gamma = 0.25, 1, 2, 6, 1, 10, 30, 60, 100$ while we keep the values of the periodic component fixed:

$$Input = A sin\left(\omega t\right) + \gamma \varepsilon_x^{1/2}\eta(t) \qquad (6)$$

In Fig.4(b) we show the maximum values of r_τ for each of the inputs as a function of γ; in Fig.4(c) we show the spectral amplitudes for the case $\gamma = 6$, black green and red are respectively the output, the input and only the noise content of the input. A dotted line is plot at the input frequency value, the presence of periodicity is completely not detectable be-
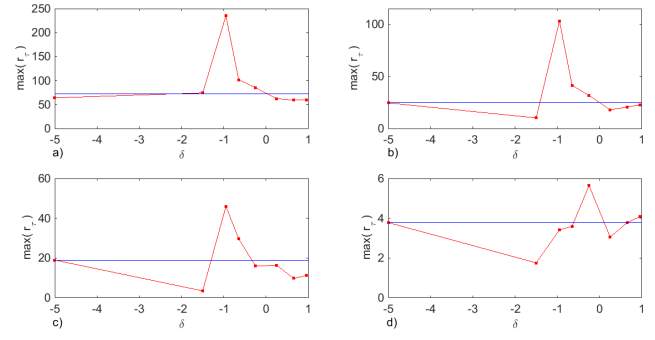
fore SR, being the difference in spectra of the noise and sine wave plus noise negligible hence the input signal before SR filtering could be characterized as white noise.

4. NUMERICAL RESULTS: THE COMPARISON

In this section we use the 2D model, system (3). The value of the variance of the Gaussian noise ε_y of the second degree of freedom will always be taken $\varepsilon_y \ll \varepsilon_x$ so that the motion will displace in the (x, y) plane but any transition in the y-mode, being the jumps between stable states of the x-mode. Firstly we test the dependence of the 2D detector on the value of the coupling constant δ with the input signal as in equation (6). We want to compare the results of this detector with the 1D one then we use same values A, ω, ε_x as in the precedent section and $\gamma = 2$. In Fig.5 we show the contour plot of r_τ for each of the T_R, S_R parameters, top left is the 1D case while all the others are the 2D case for different values of δ, respectively $\delta = -5, -1.5, -0.95, -0.65, -0.25, 0.25, 0.65, 0.95$. We notice the dependence of the position of the peaks in the (T_R, S_R) space on the value of the coupling. Furthermore due to the change on the stability of the steady states of (3) as a function of δ, we notice a difference on the area of r_τ over a threshold, i.e. the area covered by peaks visible in Fig.5. It increases with the coupling constant value varying from $-\infty < \delta < -1$ then occurs the change in the position of the steady states at $\delta = -1$ and the area covered by the peaks reaches a maximum for $\delta = -0.95$, hence for (3) approaching the case of a dynamical hysteresis [9], while decreases for $-1 < \delta < 1$. The same dependence on the coupling is found as well on the maximum values of r_τ, in Fig.6 we show such maxima as a function of δ for different values of the ratio r, plots with different vertical scales. The input signal (6) is taken for four different values of γ, respectively $\gamma = 0.25, 1, 2, 6$, while A, ω, ε_x are as in the previous simulation. We notice that the increase in the degree of synchronization of the output signal due to the 2D feature of (3) is related to the stability change in the (x, y) plane and that the maxima are found for $\delta > -1$, i.e. transitions path as in the
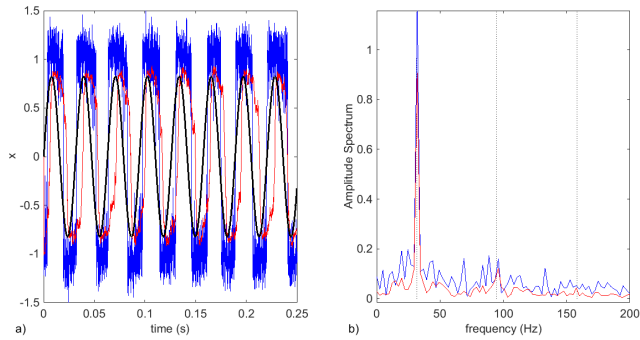
Fig. 7. comparisons of the best outputs of the 1D (blue) and 2D (red) detectors, for $\gamma = 1$, input sinusoid multiplied for a factor 3 (black): a) time signals b) amplitude spectra

red and green cases in Fig.1. The maxima of r_τ for the 1D case are blue constant lines in Fig.6, within certain values of δ we notice that the 2D detector outperforms the 1D one. In order to investigate such performance we show the comparison between the output signals of the 1D and 2D detectors for the input signal taken with $\gamma = 2$ and A, ω, ε_x as in the previous simulation. In Fig.7(a) we show the time domain, respectively blue red and black are the outputs in the 1D, 2D case and the periodic component of the input multiplied by a factor 3. Firstly we notice that in the 2D signal the variance of the output around the stable steady states is lower in respect to the one in the 1D signal; furthermore we notice that the accordance between the jumps times and the maximum values reached by the sinusoidal component is greater in the 2D case, corresponding in a fixed phase lag. In Fig.7(b) the two output signals are shown in the frequency domain, blue and red are the 1D and 2D case, dotted vertical lines are plot at the values of ω and at the first two odd harmonics. The values of the steady states in the 1D case are greater in respect to the 2D one, amplitude of output signals in Fig. 7 (a), nevertheless we notice that in the output signal of the 2D detector the power in the range 20 to 40 Hz is lower, this feature is better noticed in the first odd harmonic, which is visible in the 2D case while it is not in the 1D one; at the frequency value of 5ω the peak cannot be easily observed even in the 2D case.

5. CONCLUSION

This paper introduced a model based on a two dimensional SR mechanism for the detection of weak periodic signals, of random frequency and amplitude, buried in heavy background noise. A new measurement index was proposed, calculated directly from the vector of the zero crossing of the output signal without the need for a time-frequency transformation or *a priori* knowledge of the input signal. The new index was first shown to convey similar information to that of the signal-to-noise ratio, and was then used to evaluate the periodic content in the output signal from the SR detector. It was shown that

the presence of the coupling constant δ, used as a tuning parameter in the proposed two dimensional SR model, results in a better capacity for the detection of weak signals when compared with the usual mono-dimensional model. The best results in the two dimensional detector are found when the value of the coupling is close to $\delta = -1$ corresponding to the case of a limit cycle for the dynamics of the model. The mechanism of operation in this case appears to consist of a dynamical hysteresis where transitions occur deterministically as a function of the amplitude and frequency of the periodic forcing, and further studies are in progress to explore the nature of this mechanism. Future work will involve the experimental application of the techniques developed here in the field of condition monitoring, in particular the detection of weak fault signals in rotating machines.

REFERENCES

[1] R. Benzi, A. Sutera, and A. Vulpiani, "The mechanism of stochastic resonance," *Journal of Physics A: Mathematical and General*, vol. 14, no. 11, pp. L453, Nov. 1981.

[2] J. Lin and M.J. Zuo, "Gearbox fault diagnosis using adaptive wavelet filter," *Mechanical Systems and Signal Processing*, vol. 17, no. 6, pp. 1259–1269, Nov. 2003.

[3] J. Hongkai, H. Zhengjia, D. Chendong, and C. Peng, "Gearbox fault diagnosis using adaptive redundant lifting scheme," *Mechanical Systems and Signal Processing*, vol. 20, no. 8, pp. 1992–2006, Nov. 2006.

[4] J. Li, X. Chen, and Z. He, "Adaptive stochastic resonance method for impact signal detection based on sliding window," *Mechanical Systems and Signal Processing*, vol. 36, no. 2, pp. 240–255, Apr. 2013.

[5] Q. He, J. Wang, Y. Liu, D. Dai, and F. Kong, "Multiscale noise tuning of stochastic resonance for enhanced fault diagnosis in rotating machines," *Mechanical Systems and Signal Processing*, vol. 28, pp. 443–457, Apr. 2012.

[6] L. Barbini, I. Bordi, K. Fraedrich, and A. Sutera, "The stochastic resonance in a system of gradient type," *European Physical Journal Plus*, vol. 128, pp. 13, Feb. 2013.

[7] R. Benzi, A. Sutera, and A. Vulpiani, "Stochastic resonance in the landau-ginzburg equation," *Journal of Physics A: Mathematical and General*, vol. 18, no. 12, pp. 2239, Aug. 1985.

[8] R. Benzi and A. Sutera, "The mechanism of stochastic resonance in climate theory," in *Proceedings of the International School of Physics E. Fermi*, 1985, pp. 403–423.

[9] Jung, Gray, Roy, and Mandel, "Scaling law for dynamical hysteresis," *Physical Review Letters*, vol. 65, no. 15, pp. 1873–1876, Oct. 1990.